HEFAT2008
6th International Conference on Heat Transfer, Fluid Mechanics and Thermodynamics
30 June to 2 July 2008
Pretoria, South Africa
Paper number:HB1

COMPUTATIONAL STUDY OF BUBBLING FLUIDIZED BED

Britt M. Halvorsen[a,b], Joachim Lundberg[a], Vidar Mathiesen[c]
a. Telemark University College, Norway
b. Telemark Technological R&D Centre (Tel-Tek), Norway
c. StatoilHydro, Norway
E-mail: britt.halvorsen@hit.no

ABSTRACT

This work presents a computational study of flow behaviour in a bubbling fluidized bed. The model is developed by using the commercial CFD code Fluent 6.3. The model is based on an Eulerian description of the gas and the particle phase. Different drag models are used and compared. The computational results are validated against experimental results.

The experimental data are based on measurements performed by Britt Halvorsen in 2004. The dimension of the lab-scale fluidized bed is 0.25x0.25x2.00 m. The simulations are performed with spherical particles with mean particle size of 154 μm and density 2485 kg/m^3. The superficial gas velocity is 0.133 m/s. Computational results are compared mutually, as well as against experimental data. The discrepancies are discussed.

INTRODUCTION

Fluidized beds are widely used in industrial operations, and several applications can be found in chemical, petroleum, pharmaceutical, biochemical and power generation industries. In a fluidized bed gas is passing upwards through a bed of particles supported on a distributor. Fluidized beds are applied in industry due to their large contact area between phases, which enhances chemical reactions, heat transfer and mass transfer. The efficiency of fluidized beds is highly dependent of flow behaviour and knowledge about flow behaviour is essentially for scaling, design and optimisation.

Gravity and drag are the most dominating terms in the solid phase momentum equation. The application of different drag models significantly impacted the flow of the solid phase by influencing the predicted bed expansion and the solid concentration in the dense phase regions of the bed. Researchers have shown that their models are sensitive to drag coefficient [1-4]. In general, the performance of most current models depends on the accuracy of the drag formulation.

A number of different drag models have been proposed in modelling of fluidized beds. Ergun [5] developed a drag model that was derived empirically for Newtonian flow through packed beds in a narrow band of porosities around 0.4. In an active fluidized bed the void fraction can vary over the whole range from zero to unity and the models used in numerical simulations should be equally versatile. Gidaspow [6] combined the Ergun equation with the equations of Rowe [7] and Wen and Yu [8] to get a drag model that can cover the whole range of void fractions. Gibilaro et al. [9] proposed a model for the friction coefficient that was included in the total gas/particle drag coefficient. This model is valid for the whole range of particle concentrations. Syamlal and O'Brian [10]

NOMENCLATURE

C_D	[-]	Friction coefficient
d_s	[m]	Particle diameter
e	[-]	Coefficient of restitution
g_i	[m/s^2]	Acceleration due to gravity
g_0		Radial distribution function
K_{qm}	[kg/m^3·s]	Coefficient for the interface force between the fluid phase and the solid phase
p	[Pa]	Fluid pressure
p_s	[Pa]	Solid phase pressure
Re_s	[-]	Particle Reynolds number
U_{qi}	[m/s]	Velocity vector for phase q
v_r	[m/s]	Terminal velocity

Special characters

α_q	[-]	Volume fraction of phase q
δ_{ij}	[-]	Kroenecker delta
ρ_q	[kg/m3]	Density of phase q
$\bar{\bar{\tau}}_{ij}$	[kg/m·s^2]	Stress tensor
μ	[kg/m·s]	Viscosity
ξ_s	[kg/m·s]	Bulk viscosity
Θ_s	[m^2/s^2]	Granular temperature

Subscripts

I, j, k	I, j and k directions
g	Gas phase
s	Solid phase

have also developed an empirical drag model that that can cover the whole range of void fractions.

The success of numerical computation of bubbling fluidized beds critically depends upon the ability to handle dense packing of solids. At high solid volume fraction, sustained contacts between particles occur and the resulting frictional stresses might be accounted for in the description of the solid phase stress. Granular flows can be classified into two flow regimes, a viscous regime and a plastic regime. In a viscous or rapidly shearing regime, the stresses arise because of collisional or translational transfer of momentum, whereas in a plastic or slowly shearing regime, the stresses arise because of Coulomb friction between grains in enduring contact [11].

In the present study the Eulerian approach is used to investigate gas-solid flow in a three dimensional fluidized bed. Gidaspow drag model and the drag model of Syamlal & O'Brien are the default drag models in Fluent 6.3, and the simulations in the present study are based on these two drag models. The frictional stresses are not included in the simulations.

PHYSICAL DESCRIPTION OF BED DYNAMICS

Computational studies have been performed on a 3-dimensional fluidized bed. Spherical particles with a mean diameter of 154 µm and a density of 2485 kg/m^3 are used. The behaviour of particles in fluidized beds depends on a combination of their mean particle size and density. Geldart fluidization diagram [12], shown in Figure 1, is used to identify characteristics associated with fluidization of powders. The current particles are classified as Geldart B particles, but are very close to Geldart A particles. The fluidization properties for these two groups of particles differ significantly from each other.

Particles characterized in group A are easily fluidized and the bed expands considerably before bubbles appear. This is due to inter-particle forces that are present in group A powders [13]. Inter-particle forces are due to particle wetness, electrostatic charges and van der Waals forces. Bubble formation will occur when the gas velocity exceeds the minimum bubble velocity and the bubbles rise faster than the gas percolating through the emulsion. For group B particles the inter-particle forces are negligible and bubbles are formed as the gas velocity reaches the minimum fluidization velocity. The bubble size increases with distance above the gas distributor and increases also with increasing excess gas. The bed expansion is small compared to group A particles.

NUMERICAL METHOD

The computational work is performed by using the commercial CFD code Fluent 6.3. The model is based on an Eulerian description of the gas and the particle phase. The default settings in Fluent 6.3 are used to describe the granular phase [14]. The energy equation is not solved, and it is assumed that there is no mass transfer between the phases.

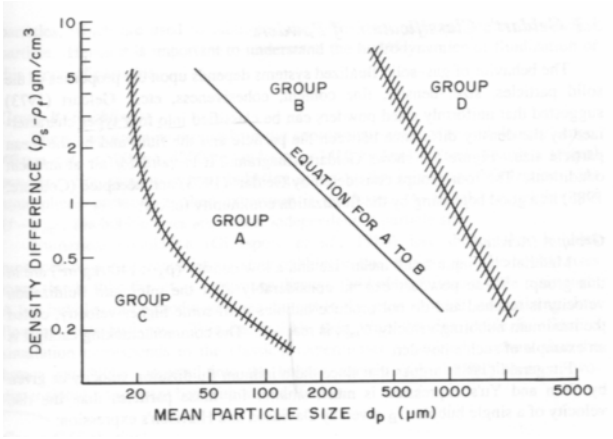

Figure 1 Geldart classification of particles according to their fluidization behaviour [12]

The continuity equation for phase q can then be expressed as:

$$\frac{\partial}{\partial t}\left(\alpha_q \rho_q\right) + \frac{\partial}{\partial x_i}\left(\alpha_q \rho_q U_{i,q}\right) = 0 \tag{1}$$

The momentum equation in the j direction for phase q is:

$$\frac{\partial}{\partial t}\left(\alpha_q \rho_q U_{j,q}\right) + \frac{\partial}{\partial x_i}\left(\alpha_q \rho_q U_{i,q} U_{j,q}\right) = -\alpha_q \frac{\partial P}{\partial x_j} + \frac{\partial \tau_{ij,q}}{\partial x_j} + \alpha_q \rho_q g_j + \sum_{m=1, m\neq q}^{M} K_{qm}\left(U_{j,m} - U_{j,q}\right) \tag{2}$$

where the terms on the lower line represent the pressure forces, viscous forces, mass forces and drag forces respectively. The gas phase stress tensor is expressed by:

$$\tau_{ij,g} = \mu_g \left[\left(\frac{\partial U_{gj}}{\partial x_i} + \frac{\partial U_{gi}}{\partial x_j}\right) - \frac{2}{3}\delta_{ij}\left(\frac{\partial U_{gk}}{\partial x_k}\right)\right] \tag{3}$$

and the solid phase stress tensor is:

$$\tau_{ij,s} = -p_s \delta_{ij} + \mu_s \left(\frac{\partial U_j}{\partial x_j} + \frac{\partial U_{si}}{\partial x_i}\right)_s + \left(\xi_s - \frac{2}{3}\mu_s\right)\delta_{ij}\left(\frac{\partial U_k}{\partial x_k}\right)_s \tag{4}$$

In the simulations the bulk viscosity is set to zero, and the solid viscosity is set constant. The solid phase pressure is modelled based on the kinetic theory of granular flow and is expressed by the following equation [14]:

$$p_s = \alpha_s \rho_s \Theta_s \left[1 + 2(1+e) g_0 \alpha_s\right] \tag{5}$$

where the terms on the right hand side represent the kinetic and the collisional contribution to the solid pressure respectively. The radial distribution function expresses the probability of collisions between the particles. The function will approach unity for dilute regions and infinity in the dense regions of the bed. The radial distribution function is given by [15]:

$$g_0 = \left[1 - \left(\frac{\alpha_s}{\alpha_{s,\max}}\right)^{\frac{1}{3}}\right]^{-1} \quad (6)$$

In a bubbling fluidized bed the concentration of particles varies from very low to very high. In dilute regions, the kinetic of the particles will dominate the solids viscosity, and the solid pressure will be close to zero. In regions with higher concentration of particles, the collisions between particles will dominate the solids viscosity, and the solid pressure will increase. At very high concentration of particles, the frictional stresses dominate the solid viscosity. In this study the frictional stresses are not accounted for.

Drag models

The drag describes the momentum exchange between phases and is expressed by the drag coefficient K_{qm} in the momentum equation. In this work two different drag models are used, The Gidaspow drag model and the Syamlal & O'Brien drag model. The Gidaspow drag model is a combination of the Ergun equation and the drag model of Wen and Yu. The Ergun equation is developed for packed beds and is only valid at high particle concentrations. To get a model that covers the whole range of particle concentrations, the Wen and Yu equation is used for the lower concentrations. The Gidaspow model for gas particle drag is:

$$K_{sg} = 150\frac{\alpha_s(1-\alpha_g)\mu_g}{\alpha_g d_s^{\,2}} + 1.75\frac{\rho_g \alpha_g \left|\vec{U}_g - \vec{U}_s\right|}{d_s} \quad (7)$$

This is the Ergun equation and is valid for $\alpha_g \leq 0.8$. The Wen and Yu equation is valid for $\alpha_g > 0.8$, and is expressed by:

$$K_{sg} = C_D \frac{3\alpha_s \alpha_g \rho_g \left|\vec{U}_g - \vec{U}_s\right|}{4 d_s} \alpha_g^{-2.65} \quad (8)$$

The friction coefficient is developed by Rowe, and is related to the Reynolds number:

$$C_D = \frac{24}{\mathrm{Re}_s}\left(1 + 0.15\,\mathrm{Re}^{0.687}\right), \qquad \mathrm{Re} \leq 1000$$
$$C_D = 0.44, \qquad \mathrm{Re} > 1000 \quad (9)$$

The Syamlal & O'Brien drag model is:

$$K_{sg} = C_D \frac{3\alpha_s \alpha_g \rho_g \left|\vec{U}_g - \vec{U}_s\right|}{4 v_r^{\,2} d_s} \quad (10)$$

The formula for the terminal velocity is developed by Garside and Al Dibuouni [14] and is an analytical formula:

$$v_r = 0.5\left(A - 0.06\,\mathrm{Re}_s + \sqrt{(0.06\,\mathrm{Re}_s)^2 + 0.12\,\mathrm{Re}_s(2B - A) + A^2}\right) \quad (11)$$

The constants A and B are:

$$A = \alpha_g^{\,4.14}$$
$$B = 0.8\alpha_g^{\,1.28}, \qquad \alpha_g \leq 0.85$$
$$B = \alpha_g^{\,2.65}, \qquad \alpha_g > 0.85 \quad (12)$$

The drag factor is proposed by Dalla Valle [14] and is expressed by:

$$C_D = \left(0.63 + \frac{4.8}{\sqrt{\mathrm{Re}_s / v_r}}\right)^2 \quad (13)$$

The granular temperature is a measurement for the random movement of the particles and influences on the solid pressure. In Fluent 6.3 there are two options for calculation of the granular temperature. The granular temperature can be described with a separate conservation equation or with an algebraic expression [14]. The algebraic expression is used in this work.

The governing equations are solved by a finite volume method, where the calculation domain is divided into a finite number of non-overlapping control volumes. The simulations are performed using three-dimensional Cartesian co-ordinates. The conservation equations are integrated in space and time. This integration is performed using first order upwind differencing in space and is fully implicit in time.

COMPUTATIONAL SET-UP

A computational study of bubble behaviour in a 3-D fluidized bed is performed. The cross section area of the bed is 0.25 m x 0.25 m and the height is 2.0 m. The initial particle height is 0.75 m, and the initial void fraction in the packed bed is 0.4. A three dimensional Cartesian co-ordinate system is used to describe the fluidized bed. The grid resolution is 10 mm in horizontal and vertical direction and the total number of control volumes is 125000. Spherical particles with a diameter of 154 μm and density 2485 kg/m^3 are used. The coefficient of restitution is set to 0.9. The boundary conditions are given as velocity inlet and pressure outlet. The inlet superficial gas velocity is set to 0.133 m/s and the outlet pressure is 1 atm. The simulations are run for about 20 s real time, and the computational results are compared to experimental data obtained on a corresponding fluidized bed with the same set-up and flow conditions. The calculated minimum fluidization velocity for particles with diameter of 154 μm and density 2485 kg/m^3 is 0.02 m/s [6], and according to Geldart fluidization diagram the particles are characterized as B particles.

RESULTS

The simulations are run with Syamlal & O'Brien drag model and with Gidaspow drag model. Figure 2 shows the mean void fraction as a function of radial position in the bed. The results are presented at height 0.39 m and 0.55 m. The results from the two drag models give no significant difference

in void fraction. Both models give lowest void fraction in the centre of the bed, and that indicates that the bubble frequency is lowest in this area. The variation in void fraction over the bed is about 0.01-0.04. Gidaspow at height 0.55 m gives the lowest variations and Gidaspow at height 0.39 m gives the highest variation.

The void fraction in the packed bed is 0.4, and according to the results shown in Figure 2, the mean void fraction in the fluidized bed is about 0.54. That means that the bed has expanded significantly, from initial bed height 0.75 m to a bed height of about 1.0 m. The mean bed height in the experimental fluidized bed was 0.85 m.

In this study the computational bubbles are defined as void fractions higher than 0.65. This definition is used because it was observed from the experimental study that parts of the bubbles can include high fractions of solids. Another reason for using a rather low void fraction in the definition of bubbles is that bubbles might occupy only a part of the control volume, and the mean void fraction for the control volume will then be lower than the void fraction in a bubble but higher than the mean void fraction in the bed. Figure 3 shows a plot of void fraction as a function of time at one position in the bed. It can be seen that the void fraction in this point varies from 0.4 to 0.77. The highest peaks represent the bubbles.

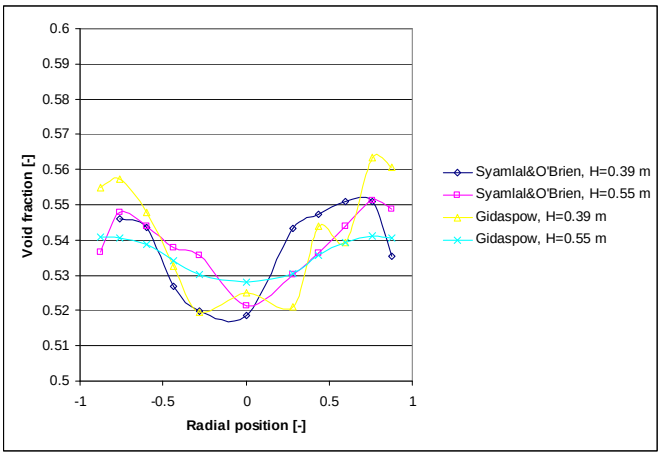

Figure 2 Void fractions as a function of radial position at different bed heights.

In Figure 4 a time series of solid volume fraction from the simulation with Syamlal & O'Brien drag model is presented. A bubble is assumed to be a region of void fraction greater than 0.80 [6]. The white areas in the fluidized bed represent void fractions greater than 0.8. It can be seen that very few bubbles satisfy this criterion. As the bed expands, the bubbles get smaller and more diffuse. After about 8 seconds the bed is stabilized at a high void fraction and only contours of small bubbles can be observed.

Figure 5 shows a comparison between the computational and experimental bubble frequency [16]. The experimental bubble frequency is significantly higher than the bubble frequencies obtained from the simulations. The Syamlal & O'Brien drag model gives slightly higher bubble frequency than the Gidaspow model.

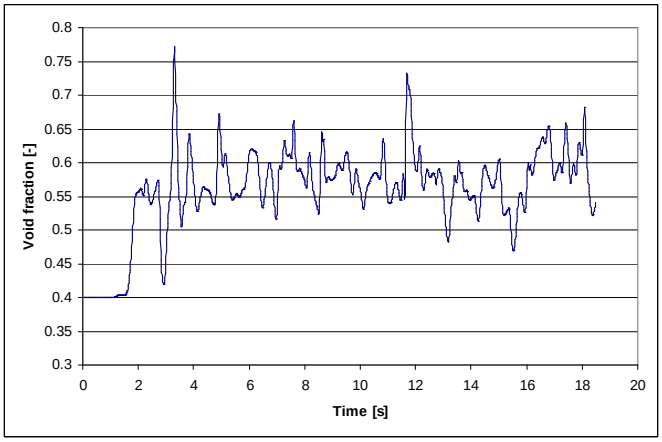

Figure 3 Bubble frequency as a function of time.

Discussion

Bubbling fluidized beds need rather long time to obtain quasi-steady state. In the experiment referred to in this work, the bubble frequency has been 1-3 bubbles per second. In the experimental study the bubble frequency was averaged over 20 minutes, whereas the computational results are averaged over 18-20 seconds due to long computational simulation time. This may explain the unsymmetrical computational void fraction profiles.

The low bubble frequencies in the simulations can be explained by the difference in the calculated and the experimental minimum fluidization velocity. The theoretical minimum fluidization velocity for spherical particles is given by:

$$U_{mf} = \frac{d_p{}^2 \Delta\rho \cdot g}{\mu} \cdot \frac{\alpha_{mf}{}^3}{1-\alpha_{mf}} \qquad (14)$$

where $\frac{\alpha_{mf}{}^3}{1-\alpha_{mf}}$ is approximately 11 [8] .

The theoretical minimum fluidization velocity for the current particles is 0.019 m/s, whereas in the experimental study, the observed minimum fluidization velocity was 0.07 m/s. In the experimental study, glass particles with a mean diameter of 154 μm were used. These particles have a particle size distribution that will influence on the flow conditions in the bed. This is not accounted for in the simulations. To account for the particle size distribution, the simulations can be run with multiple particle phases with different diameters. The particle size distribution in the experimental fluidized bed influences on the minimum fluidization velocity, and it was also observed that the particles behaved more like Geldart A particles, where the bed expands considerably before the bubbles appear. For group A particles bubbles appear as the gas velocity exceeds the minimum fluidization velocity, whereas for group B particles bubbles appear as the gas velocity reaches the minimum fluidization velocity.

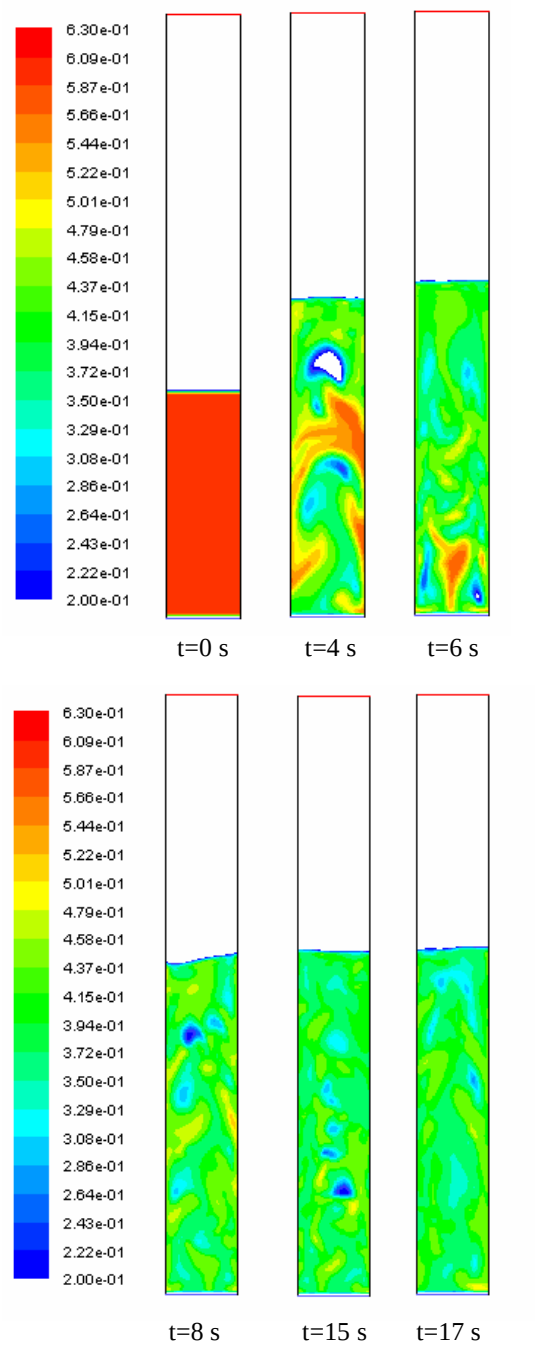

Figure 4 Volume fractions of solids. Syamlal & O'Brien drag model.

The excess gas velocity is defined as the difference between the superficial gas velocity and the minimum fluidization velocity. In the experiments, the ratio between the superficial gas velocity and the minimum fluidization velocity was about 2 whereas in the simulations this ratio is about 7. The high excess gas velocity, results in high bed expansion and thereby high mean void fraction in the bed. The conditions for bubble formations are then changed, and well defined bubbles may not appear.

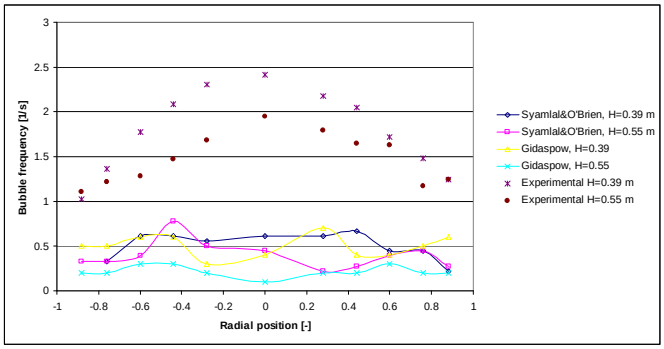

Figure 5 Bubble frequency as a function of radial position at different bed heights.

CONCLUSION

The CFD code Fluent 6.3 is used to study flow behaviour in a 3-dimensional bubbling fluidized bed. The Eulerian approach is used to describe the gas and the solid phase. The simulations are performed with Gidaspow drag model and the drag model developed by Syamlal & O'Brian. The results from the simulations with these two drag models do not differ significantly from each other. Both the models give high bed expansion, and a rather low bubble frequency. The bed expands from 0.75 m to about 1.0 m, and the bubble frequencies are about 0.5 s^{-1}. Well defined bubbles, that means a region of void fraction greater than 0.80, are only observed in the first 4 seconds. The Syamlal & O'Brian drag model gives slightly higher bubble frequency than the Gidaspow drag model.

The simulations are compared to experimental results. The experimental study is performed with spherical glass particles with mean particle size of 154 µm and density 2485 kg/m^3. The initial particle height is 0.75 m and the superficial gas velocity is 0.133 m/s. The same conditions are used for the simulations. In the experiments, however, the particles have a size distribution that covers particle sizes from about 50 µm to 250 µm. In the simulation all the particles are defined with the same diameter, 154 µm. The simulations give considerably lower bubble frequencies than the experiments. The experimental bubble frequency is about2 s^{-1}, and that is about 4 times the bubble frequencies obtained in the simulations. The bed expansion in the experiments is about 0.1 m, whereas it is about 0.25 m in the simulations. The discrepancies between computational and experimental result may be due to the different ranges of particle sizes. The observed experimental minimum fluidization velocity is about 4 times the calculated minimum fluidization velocity for particles with diameter 154 µm. The consequence of this is that the excess gas velocity becomes much higher in the simulations than in the experiments, and the ideal conditions for a bubbling fluidized bed might no longer be present. To get a better agreement between simulations and experiments, the simulations should be performed with multiple particle phases to account for the particle size distribution in the experiments.

REFERENCES

[1] Yasuna, J.A., Moyer, H.R., Elliott, S., Sinclair, J.L. (1995), Qantitative predictions of gas-particle flow in vertical pipe with particle-particle interactions, *Powder Technology* **84**, pp. 23-34.

[2] Halvorsen, B., Mathiesen, V. (2002), CFD Modelling and simulation of a lab-scale Fluidised Bed, *Modeling, Identification and Control*, **23**(2), pp. 117-133.

[3] Ibsen, C.H. (2002), An experimental and Computational Study of Gas-Particle Flow in Fuidised Reactors, Ph.D. Thesis, Aalborg University, Esbjerg.

[4] Bokkers, G.A., van Sint Annaland, M., Kuipers, J.A.M. (2004), Mixing and segregation in a bidiperse gas-solid fluidised bed: a numerical and experimental study, *Powder Technology*, **140**, pp. 176-186.

[5] Ergun, S. (1952), Fluid Flow Through Packed Columns, *Chemical Engineering Progress*, **48**(2), pp. 89-94.

[6] Gidaspow, D. (1994), Multiphase Flow and Fluidization. Academic Press, Boston

[7] Rowe, P.N. (1961), Drag Forces in a Hydraulic Model of Fluidized Bed-PartII, *Trans. Instn. Chem.*, **39**, pp. 175-180.

[8] Wen, C.Y., Yu, Y.H. (1966), Mechanics of Fluidization, *Chemical Engineering Progress*, **62**, pp. 100-111.

[9] Gibilaro, L.G., Di Felice, R., Waldram, S.P. (1985), Generalized Friction Factor and Drag Coefficient for Fluid-Particle Interaction, *Chemical Engineering Science*, **40(10)**, pp. 1817-1823.

[10] Syamlal, M., O'Brien, T.J. (1987), A Generalized Drag Correlation for Multiparticle Systems, Morgantown Energy Technology Center, DOE Report.

[11] Jenkins, J.T., Cowin, S.C. (1979), Theories for Flowing Granular Materials, Mech. Applied to Transport of Bulk Materials, *Ap. Mech.Div. of ASME*, 31, pp. 79-89.

[12] Geldart, D. (1973), Types of Gas Fluidization, *Powder Technology*, 7, pp 285-295.

[13] Geldart, D. (1986), Gas Fluidization Technology, John Wiley & Sons Ltd.

[14] Fluent, Fluent 6.2 Users Guide, *Fluent Inc., Lebanon, NH, USA*, 2005.

[15] Bagnold, R.A. (1954), Experiments on a Gravity-Free Dispersion of Large Solid Spheres in a Newtonian Fluid Under Shear. *Proc. of Roy. Soc.*, **A225**, pp. 49-63.

[16] Halvorsen, B., An experimental and computational study of flow behaviour in bubbling fluidized beds, Doctoral Thesis at NTNU: 70, 2005.